

Impaired functional integration in multiple sclerosis: a graph theory study

Maria A. Rocca · Paola Valsasina · Alessandro Meani ·
Andrea Falini · Giancarlo Comi · Massimo Filippi

Received: 14 April 2014 / Accepted: 19 September 2014 / Published online: 26 September 2014
© Springer-Verlag Berlin Heidelberg 2014

Abstract Aim of this study was to explore the topological organization of functional brain network connectivity in a large cohort of multiple sclerosis (MS) patients and to assess whether its disruption contributes to disease clinical manifestations. Graph theoretical analysis was applied to resting state fMRI data from 246 MS patients and 55 matched healthy controls (HC). Functional connectivity between 116 cortical and subcortical brain regions was estimated using a bivariate correlation analysis. Global network properties (network degree, global efficiency, hierarchy, path length and assortativity) were abnormal in MS patients vs HC, and contributed to distinguish cognitively impaired MS patients (34 %) from HC, but not the main MS clinical phenotypes. Compared to HC, MS patients also showed: (1) a loss of hubs in the superior frontal gyrus, precuneus and anterior cingulum in the left hemisphere; (2) a different lateralization of basal ganglia hubs (mostly located in the left hemisphere in HC, and in the right hemisphere in MS patients); and (3) a formation

of hubs, not seen in HC, in the left temporal pole and cerebellum. MS patients also experienced a decreased nodal degree in the bilateral caudate nucleus and right cerebellum. Such a modification of regional network properties contributed to cognitive impairment and phenotypic variability of MS. An impairment of global integration (likely to reflect a reduced competence in information exchange between distant brain areas) occurs in MS and is associated with cognitive deficits. A regional redistribution of network properties contributes to cognitive status and phenotypic variability of these patients.

Keywords Multiple sclerosis · Graph analysis · Resting state fMRI · Cognitive impairment · Phenotype

Introduction

The human brain is a complex network of interacting regions connected by white matter tracts. The characterization of structural and functional features of such a network in healthy subjects and diseased people has the potential to improve our understanding of the pathophysiology and clinical manifestations of many neurological and psychiatric conditions (Filippi et al. 2013). This has led to the use of new tools for complex system analysis to tackle brain diseases (Bullmore and Sporns 2009). Among these, graph theory is a mathematical framework which allows to describe a network as a graph, consisting of a collection of nodes (i.e., brain regions) and edges (i.e., structural and functional connections) (Bullmore and Sporns 2009; Rubinov and Sporns 2010). Using graph theory, distinct modifications of brain network topology have been identified during development and normal ageing, and disrupted functional and structural connectivities have been

M. A. Rocca · P. Valsasina · A. Meani · M. Filippi (✉)
Neuroimaging Research Unit, Division of Neuroscience,
Institute of Experimental Neurology, San Raffaele Scientific
Institute, Vita-Salute San Raffaele University, Via Olgettina,
60, 20132 Milan, Italy
e-mail: filippi.massimo@hsr.it

M. A. Rocca · G. Comi · M. Filippi
Department of Neurology, San Raffaele Scientific Institute,
Vita-Salute San Raffaele University, Milan, Italy

A. Falini
Department of Neuroradiology, San Raffaele Scientific Institute,
Vita-Salute San Raffaele University, Milan, Italy

A. Falini
CERMAC, San Raffaele Scientific Institute, Vita-Salute San
Raffaele University, Milan, Italy

associated with several neurological and psychiatric conditions, including dementia, amyotrophic lateral sclerosis, and schizophrenia (Filippi et al. 2013). In the latter, connectomic approaches have contributed to prove the theory of this condition as a disconnection syndrome (Filippi et al. 2013).

In multiple sclerosis (MS), the occurrence of disconnection has been substantiated by structural MRI studies of brain network topology (He et al. 2009; Li et al. 2013; Shu et al. 2011), which showed a decreased structural connectivity of regions of the fronto-temporal lobes. At present, functional abnormalities of brain network topology have been investigated only marginally in this condition (Schoonheim et al. 2011).

By applying graph analysis to resting state (RS) fMRI data, we investigated the topological organization of the functional brain connectome in a large cohort of MS patients. Our working hypothesis was that the disruption of brain network functional connectivity at a global and regional level is likely to contribute to the clinical manifestations of the disease, especially cognitive impairment.

Materials and methods

Subjects

We recruited consecutively 246 right-handed MS patients (Polman et al. 2011) (85/161 men/women, mean age = 42.3 years, range = 19–60 years). One hundred and twenty-one patients (44/77 men/women) had relapsing remitting (RR) MS (Lublin and Reingold 1996), 45 (10/35 men/women) benign MS (BMS) [Expanded Disability Status Scale (EDSS) score ≤ 3.0 after a disease duration of at least 15 years] (Hawkins and McDonnell 1999) and 80 (31/49 men/women) secondary progressive (SP) MS (Lublin and Reingold 1996). To be included, patients had to: (1) be relapse- and steroid free for at least 3 months before the fMRI experiment; (2) have no significant medical illnesses or substance abuse that could interfere with cognitive functioning; and (3) have no other major systemic, psychiatric or neurological diseases.

All patients underwent a complete neurologic examination within 2 days of the MRI study, with rating of the EDSS score. As a measure of cognitive impairment, we used the paced auditory serial addition test (PASAT), which is sensitive to abnormalities of working memory and information processing speed. This test is accepted as the reference test for cognitive assessment as part of the MA functional composite score in MS (Fischer et al. 1999). Patients were considered cognitively impaired (CI) when

PASAT score was 2SD below the average score of a comparable control group for age, gender and education (Amato et al. 2006).

Fifty-five right-handed, age- and gender-matched healthy controls (HC) (19/36 men/women, mean age = 41.7 years, range = 20–60 years) with no previous history of neurological, psychiatric, or medical disorders, and a normal neurological exam were also enrolled. Table 1 summarizes the main demographic, clinical and conventional MRI characteristics of the different study groups.

Ethics committee approval

Approval was received from the local ethical standards committee on human experimentation, and written informed consent was obtained from all subjects prior to enrolment.

MRI acquisition

Using a 3.0 T Philips Intera scanner, the following sequences of the brain were acquired from all subjects during a single session: (a) T2*-weighted single-shot echo planar imaging (EPI) sequence for RS fMRI [repetition time (TR) = 3,000 ms, echo time (TE) = 35 ms, flip angle = 90°, field of view (FOV) = 240 mm²; matrix = 128 × 128, slice thickness = 4 mm, 200 sets of 30 contiguous axial slices, parallel to the AC-PC plane]. Positioning of RS fMRI scans was carefully performed to include the entire cerebellum/pons region; (b) dual-echo turbo spin echo (TSE) [TR/TE = 3,500/24–120 ms; flip angle = 150°; FOV = 240 mm²; matrix = 256 × 256; echo train length (ETL) = 5; 44 contiguous, 3-mm-thick axial slices]; and (c) 3D T1-weighted fast field echo (TR = 25 ms, TE = 4.6 ms, flip angle = 30°, FOV = 230 mm², matrix = 256 × 256, slice thickness = 1 mm, 220 contiguous axial slices, in-plane resolution = 0.89 × 0.89 mm²). Total acquisition time of RS fMRI was about 10 min. During scanning, subjects were instructed to remain motionless and not to think anything in particular. All subjects reported that they had not fallen asleep during scanning, according to a questionnaire delivered immediately after the MRI session.

Conventional MRI analysis

T2 hyperintense lesion volume (LV) was quantified by one experienced observer, unaware of patient's identity, using a local thresholding segmentation technique (Jim 5, Xinapse Systems Ltd., Northants, UK). Normalized brain volume (NBV) was calculated from 3D T1-weighted images (Smith 2002).

Table 1 Main demographic, clinical and conventional MRI characteristics of healthy subjects and patients with MS

	Healthy subjects	MS patients	<i>p</i> *	CP MS patients	CI MS patients	RRMS patients	BMS patients	SPMS patients	<i>p</i> **
Mean age, years (range)	41.7 (20–60)	42.3 (19–60)	0.2	40.4 (19–59)	48.1 (27–60)	39.5 (19–59)	45.0 (33–60)	48.1 (26–60)	<0.001
Mean disease duration, years (range)	–	13.7 (0–36)	–	12.4 (1–33)	16.1 (0–36)	9.1 (0–13)	20.2 (15–33)	17.1 (3–36)	<0.001
Median EDSS (range)	–	3.0 (0.0–9.0)	–	2.0 (0.0–8.0)	4.0 (1.0–9.0)	2.0 (0.0–4.5)	2.0 (0.0–3.0)	6.0 (4.0–9.0)	<0.001 [§]
T2 lesion volume, ml (SD)	–	12.6 (13.2)	–	9.5 (10.2)	17.5 (15.6)	7.9 (8.6)	13.7 (11.8)	19.1 (16.6)	<0.001
Normalized brain volume, ml (SD)	1,576 (86)	1,452 (105)	<0.001	1,483 (90)	1,401 (105)	1,486 (97)	1,437 (88)	1,393 (104)	<0.001

SD standard deviation, EDSS Expanded Disability Status Scale, CI cognitively impaired, CP cognitively preserved, RR relapsing remitting, BMS benign form of MS, SP secondary progressive
 * Two-sample *t* test; ** ANOVA model; † Mann–Whitney test; ‡ Kruskal and Wallis test

RS fMRI data pre-processing

All fMRI analyses were performed by an experienced observer, unaware of subject's identity. Using Statistical Parametric Mapping (SPM8), RS fMRI images were realigned to the mean of each session with a six degree rigid-body transformation to correct for minor head movements. The mean cumulative translations were 0.11 mm (SD 0.22 mm) for HC and 0.13 mm (SD 0.24 mm) for MS patients ($p = 0.3$). Mean translations were 0.13 mm (SD 0.24) for CP and 0.12 mm (SD 0.24) for CI MS patients ($p = 0.8$). The mean rotations were $<0.1^\circ$ in all groups ($p = 0.3$). Data were normalized to the SPM8 default EPI template using a standard affine followed by a non-linear transformation (Ashburner and Friston 1999), and band-pass filtered between 0.01 and 0.08 Hz using the REST software (<http://resting-fmri.sourceforge.net/>) to partially remove low-frequency drifts and physiological high-frequency noise. Using REST, non-neuronal sources of synchrony between RS fMRI time series and motion-related artifacts were minimized by regressing out the six motion parameters estimated by SPM8 (Lund et al. 2005), and the average signals of the ventricular cerebrospinal fluid and white matter. The removal of the average signal from the cerebrospinal fluid, which is highly correlated with physiological noise, is likely to improve dramatically the reliability of the RS fMRI measurements, especially from cerebellar regions (Diedrichsen et al. 2010). No spatial smoothing was applied, to avoid spurious correlations between neighbouring voxels, as previously suggested (Sanz-Arigita et al. 2010).

Construction of functional brain networks

To construct functional brain networks, we employed an automated anatomical labelling (AAL) atlas (Tzourio-Mazoyer et al. 2002) to parcel the brain into 116 cortical and subcortical regions of interest (ROI). Time series were extracted from each ROI by averaging the signal from all voxels within each region. Bivariate correlations between each ROI pair were obtained by calculating the Pearson's correlation coefficient between ROI time courses. These correlation coefficients represent functional connectivity strengths between brain regions. Correlation matrices obtained from all study subjects were thresholded into binary connectivity matrices at different correlation thresholds (τ , resulting in unweighted graphs with the nodes representing brain regions and edges/links representing functional relationships between brain regions) (Rubinov and Sporns 2010). The number of connections surviving at a given correlation threshold can vary between subjects: in other words, even when fixing τ graphs from different subjects might have a different number of

significant links. Therefore, previous studies did not use a fixed τ for all study subjects, but instead defined the so-called network sparsity, essentially meaning that they forced the total number of existing connections to be the same for all study subjects (de Haan et al. 2009; He et al. 2008; Tian et al. 2011; Yao et al. 2010). Such an approach may lead to inaccurate results, since fixing a pre-defined sparsity may result in a modification of network topology (van Wijk et al. 2010). For instance, in networks with low average connectivity, a consistent number of not significant correlation values might be converted into significant connections to achieve the imposed network degree; in contrast, in networks with high average connectivity, a large number of significant correlations might be ignored (van Wijk et al. 2010). Therefore, as performed in previous studies (Meunier et al. 2009; Salvador et al. 2005; van den Heuvel et al. 2009), we chose to construct our graphs by fixing the same τ for all study subjects. Because there is no definitive method for choosing τ we examined several possible network configurations for a range of τ values ranging from 0 to 0.9 (excluding negative correlations), and explored the consistency of results over this range (Sanz-Arigita et al. 2010). Then, we explored network characteristics only over the range of thresholds that yielded not disconnected graphs ($0 \leq \tau \leq 0.20$, with increments of 0.01). Table 2 reports the number of subjects showing graph disconnectivity as a function of increasing correlation threshold τ . For MS patients, the corresponding median EDSS score is provided. The range of selected correlation thresholds is close to values which were demonstrated to provide the best trade-off between a low positive false discovery rate (FDR) (Benjamini and Hochberg 1995) and false non-discovery rate for functional connectivity matrices (Sala et al. 2014).

Network analysis

Global and regional network properties were explored using the Brain Connectivity Matlab toolbox (<http://www.brain-connectivity-toolbox.net>) (Rubinov and Sporns 2010).

Global network analysis Six global network metrics, including two small-world measures [i.e., clustering coefficient (C) and characteristic path length (L)] (Watts and Strogatz 1998), mean network degree, global efficiency (Latora and Marchiori 2001), assortativity, and hierarchy (Bassett et al. 2008) were explored. The clustering coefficient (C) of a node is the number of links existing between its nearest neighbours and represents the fraction of the node's neighbours that are also neighbours of each other (Watts and Strogatz 1998). In turn, the mean network C represents how strongly a given network is locally interconnected. The characteristic path length (L) is defined

Table 2 Number of subjects showing graph disconnectivity as a function of increasing correlation threshold τ

Correlation threshold τ range	Number of subjects showing graph disconnectivity (%)		Median EDSS score (range)
	Controls	MS patients	
$0 < \tau \leq 0.10$	0 (0)	0 (0)	–
$0.10 < \tau \leq 0.20$	0 (0)	0 (0)	–
$0.20 < \tau \leq 0.30$	4 (7)	32 (13)	2.0 (1.0–8.0)
$0.30 < \tau \leq 0.40$	17 (31)	101 (41)	4.0 (0.0–9.0)
$0.40 < \tau \leq 0.50$	20 (37)	89 (36)	2.5 (0.0–8.5)
$0.50 < \tau \leq 0.60$	12 (22)	22 (9)	2.5 (0.0–8.0)
$\tau > 0.60$	2 (3)	2 (1)	4.0 (3.5–4.5)

For patients with MS, the corresponding median Expanded Disability Status Scale (EDSS) score is provided

MS multiple sclerosis, EDSS Expanded Disability Status Scale

as the average shortest path length between all pairs of nodes in the same network (Watts and Strogatz 1998). Since L represents the average number of nodes that have to be crossed to go from one node to any other node, it is taken as a measure of functional integration. The degree (k) of a single node is the number of links connected to that node. The mean network degree is the average degree of all network nodes, and is a measure of network density (Rubinov and Sporns 2010). Global efficiency is the average inverse shortest path length (Latora and Marchiori 2001) and is a measure of the overall information transfer efficiency across the whole network. Assortativity, also known as degree correlation (Newman 2002), is a measure of correlation between nodal degree and mean degree of its nearest neighbours, obtained by averaging the correlation coefficients of the degrees of every connected node pair (Newman 2002). Positive assortativity values indicate that nodes are likely to be connected to other nodes with the same degree and, therefore, that high-degree nodes or hubs of the network are likely connected to each other. Finally, the hierarchical structure of our networks was quantified by the β coefficient, which is a parameter of the power-law relationship between C and k of the nodes in the network (Ravasz and Barabasi 2003): $C = k^{-\alpha}$. We estimated α by fitting a linear regression line to the plot of $\log(C)$ versus $\log(k)$ for the network.

Networks having small-worldness properties were defined as those significantly more clustered than random networks, but having approximately the same characteristic path length. To assess small-worldness, we computed the normalized clustering coefficient $\gamma = C_{\text{real}}/C_{\text{rand}}$, and the normalized characteristic path length $\lambda = L_{\text{real}}/L_{\text{rand}}$ (Watts and Strogatz 1998), where C_{real} and L_{real} were clustering coefficients and characteristic path lengths of the average

brain networks of each study group, and C_{rand} and L_{rand} represented the corresponding indices calculated on 100 matched random networks preserving the same numbers of nodes, edges, and degree distribution as the observed average network (Maslov and Sneppen 2002). By definition, a small-world network has $\gamma > 1$ and $\lambda \approx 1$ (Watts and Strogatz 1998). These two measurements can be summarized into a simple quantitative metric, small-worldness, $\sigma = \gamma/\lambda > 1$ (Humphries et al. 2006).

Hubs and regional network analysis Hubs were identified on the basis of centrality in the network. We used two metrics of nodal centrality: nodal degree and betweenness centrality. Degree, the number of links connected to a node, is one of the most common measures of centrality. Betweenness centrality is the fraction of all shortest paths in the network that pass through a given node (Rubinov and Sporns 2010); therefore, bridging nodes, that connect disparate parts of a network, result in a high betweenness centrality. Degree and betweenness centrality were calculated for every threshold (τ) that yielded not disconnected graphs (i.e., between 0 and 0.20). Then, the two nodal parameters X_{nod} (degree and betweenness centrality) were obtained by integrating over all considered thresholds (Tian et al. 2011). A brain region was defined as a hub when X_{nod} of any of its two nodal metrics was at least 1 SD higher than the average of the corresponding parameter over the entire network (Tian et al. 2011).

Sample size calculation

The main aim of this study is the comparison of network measures (i.e., degree, clustering coefficient, path length, efficiency, assortativity and hierarchy) between healthy controls ($N = 55$) and MS patients ($N = 246$). Assuming a type I error (alpha) of 0.05, our study is powered at 90 % to detect a statistical significant difference for each network measure, equal between groups to a Cohen-standardized effect size of 0.5.

Statistical analysis

Brain T2 lesion volumes (LV) were log-transformed before statistical analysis due to their skewed distribution. Kolmogorov–Smirnov test was used to verify Gaussianity of distribution of demographic, clinical, conventional MRI and network metrics. Variables following a Gaussian distribution (i.e., age, disease duration, log T2 LV, NBV and all global network measures) were compared between groups using two-sample t tests or ANOVA models, as appropriate. Categorical variables (i.e., EDSS, the presence/absence of cognitive impairment and regional network measures) were compared between groups using the Mann–Whitney and the Kruskal–Wallis tests, as

appropriate. For all these measures, the following between-group comparisons were decided a priori: (1) HC vs MS patients (as a whole), (2) HC vs CP and CI patients, and (3) HCs vs RRMS, RRMS vs SPMS, RRMS vs BMS, and SPMS vs BMS (decided on the basis of the clinical evolution of the disease).

ANOVA models, adjusted for age and gender, were used to compare global network properties between groups. The analysis was repeated by correcting p values for multiple comparisons over the different correlation thresholds τ with the FDR approach (Benjamini and Hochberg 1995). To investigate the effect of gender, network metrics were also compared between male/female HCs and male/female MS patients using 2×2 ANOVA models adjusted for age.

A Mann–Whitney test was used to compare integrated nodal parameters (X_{nod}) of degree and betweenness centrality from all 116 automated anatomical labelling (AAL) atlas (Tzourio-Mazoyer et al. 2002) regions between study groups. Correction for multiple comparisons was performed by applying a modified version of FDR, called positive FDR (pFDR) (Storey 2003). While the traditional FDR approach involves a sequential p value rejection method based on the observed data (Benjamini and Hochberg 1995), by fixing the error rate and estimating the corresponding region of rejection, the pFDR method applies the opposite strategy, i.e., a rejection region is fixed and the corresponding error rate is estimated (Storey 2003). This approach, statistically more powerful than FDR (Storey 2003), allows to control for multiple comparisons and ranks brain regions according to their importance in explaining between-group differences. Ranked significance is measured by the q value, the pFDR analogue of the p value (Storey 2003). We considered statistically significant only brain regions associated with an error rate smaller than 0.1 % (i.e., $q \leq 0.001$).

The relationships of global and regional network properties with conventional MRI measures were tested using linear regression models with age and gender as confounding covariates.

Results

Clinical and conventional MRI measures

Thirty-four percent of MS patients were CI. Compared to cognitively preserved (CP), CI MS patients were significantly older, had longer disease duration, higher EDSS and T2 LV, and lower NBV. The proportion of CI patients was higher in SPMS than RRMS (50 vs 23 %, $p < 0.001$), while it did not differ between BMS and RRMS (37 vs 23 %, $p = 0.34$). Disease duration was longer in BMS vs

Table 3 Small-worldness metrics γ , λ and σ in healthy controls and MS patients over the range of correlation thresholds examined

Correlation thresholds	Groups	γ	λ	σ
0.00	Healthy controls	1.003	1	1.003
	MS patients	1.005	1	1.005
	CP MS patients	1.003	1	1.003
	CI MS patients	1.006	1	1.006
	RRMS patients	1.004	1	1.004
	BMS patients	1.005	1	1.005
	SPMS patients	1.005	1	1.005
0.05	Healthy controls	1.007	1	1.007
	MS patients	1.009	1	1.009
	CP MS patients	1.007	1	1.007
	CI MS patients	1.011	1	1.011
	RRMS patients	1.007	1	1.007
	BMS patients	1.010	1	1.010
	SPMS patients	1.010	1	1.010
0.10	Healthy controls	1.014	1	1.014
	MS patients	1.017	1.001	1.016
	CP MS patients	1.014	1.001	1.013
	CI MS patients	1.019	1.001	1.018
	RRMS patients	1.014	1.001	1.013
	BMS patients	1.019	1.001	1.018
	SPMS patients	1.019	1.001	1.018
0.15	Healthy controls	1.025	1.001	1.024
	MS patients	1.030	1.002	1.028
	CP MS patients	1.024	1.002	1.022
	CI MS patients	1.033	1.002	1.031
	RRMS patients	1.025	1.001	1.023
	BMS patients	1.032	1.002	1.030
	SPMS patients	1.034	1.002	1.031
0.20	Healthy controls	1.043	1.001	1.041
	MS patients	1.050	1.005	1.044
	CP MS patients	1.041	1.004	1.036
	CI MS patients	1.053	1.006	1.046
	RRMS patients	1.042	1.004	1.037
	BMS patients	1.054	1.005	1.048
	SPMS patients	1.053	1.005	1.047

Small-worldness properties are verified when networks are significantly more clustered than random networks (i.e., $\gamma > 1$), but have approximately the same characteristic path length as random networks (i.e., $\lambda \approx 1$). These two measures can be summarized in a simple metric, $\sigma (= \gamma/\lambda) > 1$

γ normalized clustering coefficient, λ normalized characteristic path length, *CP* cognitively preserved, *CI* cognitively impaired, *RR* relapsing remitting, *BMS* benign form of MS, *SP* secondary progressive

SPMS ($p = 0.004$) and RRMS ($p < 0.001$) patients, and SPMS vs RRMS ($p < 0.001$) patients. T2 LV was significantly higher in SPMS and BMS vs RRMS patients ($p < 0.001$ and 0.001). NBV was significantly lower in

SPMS vs RRMS ($p < 0.001$) and BMS ($p = 0.03$) and in BMS vs RRMS patients ($p = 0.009$).

Global network analysis

Small-worldness was verified in HCs and MS patients (as a whole and in the different study subgroups) (Table 3). The majority of graph theoretical metrics were significantly abnormal in MS patients compared to HCs (Fig. 1; Table 4), especially at low correlation thresholds. Mean network degree, global efficiency, and hierarchy were lower (p values ranging from 0.01 to 0.05), and path length and assortativity higher (p values ranging from <0.001 to 0.05) in MS patients (Fig. 1; Table 4). No effect of gender was detected.

Regional network analysis

Hub regions

Table 5 and Fig. 2 report hubs in HCs and MS patients. The bilateral cerebellum (crus I), left cerebellum (crus II), right anterior cingulate cortex (ACC), right orbitofrontal cortex, bilateral inferior and middle temporal gyrus, and bilateral middle cingulate cortex were hubs in both groups. The left precuneus, superior frontal gyrus (SFG) and ACC were hubs in HCs, only. The left superior temporal pole and cerebellar lobule IV–V were hubs in MS patients, only. Basal ganglia hubs were mostly located in the left hemisphere in HCs, and in the right hemisphere in MS patients.

Regional nodal characteristics

Compared with controls, MS patients showed a significantly lower nodal degree in the bilateral caudate nucleus and right cerebellum (crus I) (Table 6). Betweenness centrality did not differ between MS patients and HCs.

Network analysis and cognitive impairment

Global network analysis

Compared to HCs and CP patients, CI MS patients had lower mean network degree, global efficiency and hierarchy (p values ranging from 0.002 to 0.02) and higher path length (p values ranging from 0.002 to 0.01) at several correlation thresholds (Fig. 3; Table 4). No differences were found between CP MS patients and HCs.

Regional network analysis

Table 5 and Fig. 2 report hubs in CP and CI MS patients. Hubs in CP MS patients were similar to those described for

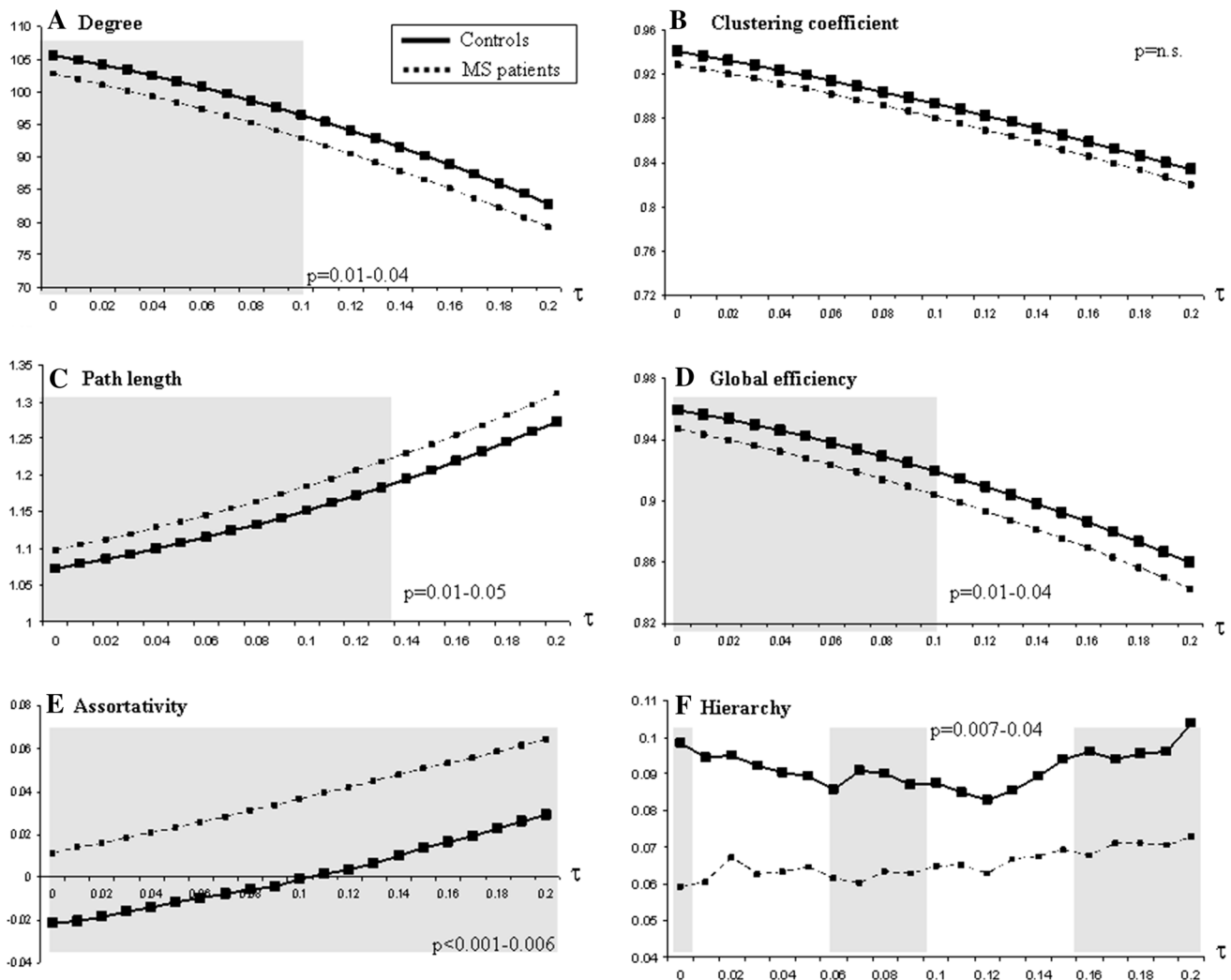


Fig. 1 Plots of global network properties in healthy controls (*black line*) and patients with MS (*black dashed line*) over the selected range of correlation thresholds τ : **a** mean network degree; **b** clustering coefficient; **c** characteristic path length; **d** global efficiency;

e assortativity; and **f** hierarchy. See text for further details. *Shade areas* indicate the range of thresholds where between-group differences were statistically significant

the whole group of MS patients except for the presence of additional hubs in the lobule VIII of the right cerebellum, the left orbitofrontal cortex and left caudate nucleus. A preservation of the thalamic and ACC hubs in the left hemisphere was also detected. Differently from HCs and CP patients, CI MS patients did not have hubs in the left frontal cortex. They also showed no thalamic hubs (Table 5; Fig. 2).

Compared to HCs, both CP and CI MS patients showed significantly lower nodal degree in the bilateral caudate nucleus. CI MS patients also showed a decreased nodal degree in the right cerebellum (crus I and lobule VIII), left ACC, left SFG, left precuneus and left thalamus (Table 6). No differences were found between CP and CI MS patients. Betweenness centrality did not differ between groups.

Network analysis and MS clinical phenotype

Global network analysis

At low correlation thresholds, mean network degree, global efficiency, path length, and assortativity were significantly different between MS phenotypes (p values ranging from <0.001 to 0.05 ; Table 4). At post hoc analysis, no significant differences were found between MS phenotypes.

Regional network analysis

Figure 4 and Table 7 report hubs in the different MS clinical phenotypes. Hubs in HCs are also reported for clarity. The left superior temporal pole and right basal ganglia were hubs in all MS clinical phenotypes. In

Table 4 Average values and standard deviations (SD) of global network parameters in healthy controls (HC) and patients with MS as a whole and in the different study subgroups

Metric	Correlation threshold	Healthy controls	MS patients	<i>p</i> *	CP MS patients	CI MS patients	<i>p</i> *	RRMS patients	SPMS patients	BMS patients	<i>p</i> *
Mean network degree (SD)	0.00	105.5 (6.5)	102.7 (7.0)	0.01[§]	103.9 (6.6)	100.9 (7.1)	0.006[§]	103.9 (6.8)	101.6 (7.2)	101.3 (6.5)	0.02
	0.03	103.3 (7.6)	100.1 (8.2)	0.01[§]	101.6 (7.8)	98.1 (8.2)	0.009[§]	101.5 (8.0)	98.9 (8.5)	98.6 (7.6)	0.03
	0.06	100.6 (8.9)	97.2 (9.5)	0.02[§]	98.9 (9.1)	94.9 (9.4)	0.01[§]	98.8 (9.2)	95.8 (10.0)	95.4 (8.8)	0.04
	0.09	97.5 (10.2)	94.0 (10.8)	0.04	95.9 (10.5)	91.4 (10.6)	0.01[§]	95.8 (10.5)	92.5 (11.5)	92.0 (9.9)	0.06
	0.12	94.0 (11.6)	90.4 (12.3)	0.07	92.6 (11.8)	87.5 (11.9)	0.01[§]	92.3 (11.9)	88.7 (13.1)	88.1 (11.1)	0.09
	0.15	90.1 (12.9)	86.4 (13.7)	0.10	88.8 (13.3)	83.2 (13.2)	0.02[§]	88.6 (13.2)	84.6 (14.6)	83.9 (12.4)	0.11
Clustering coefficient (SD)	0.18	85.8 (14.2)	82.1 (15.0)	0.14	84.7 (14.7)	78.7 (14.4)	0.03[§]	84.4 (14.5)	80.3 (16.2)	79.4 (13.6)	0.15
	0.20	82.7 (15.0)	79.1 (15.8)	0.17	81.8 (15.6)	75.6 (15.1)	0.03[§]	81.4 (15.3)	77.3 (17.1)	76.2 (14.4)	0.17
	0.00	0.94 (0.04)	0.93 (0.04)	0.12	0.93 (0.04)	0.91 (0.04)	0.04	0.93 (0.04)	0.92 (0.05)	0.92 (0.05)	0.17
	0.03	0.92 (0.05)	0.91 (0.05)	0.16	0.92 (0.05)	0.90 (0.05)	0.06	0.92 (0.05)	0.91 (0.05)	0.90 (0.05)	0.19
	0.06	0.91 (0.05)	0.90 (0.06)	0.21	0.91 (0.05)	0.88 (0.06)	0.07	0.91 (0.05)	0.89 (0.06)	0.89 (0.05)	0.22
	0.09	0.89 (0.06)	0.88 (0.06)	0.25	0.89 (0.06)	0.87 (0.06)	0.07	0.89 (0.06)	0.87 (0.07)	0.87 (0.06)	0.24
Path length (SD)	0.12	0.88 (0.07)	0.87 (0.07)	0.29	0.88 (0.07)	0.85 (0.07)	0.07	0.87 (0.06)	0.86 (0.07)	0.86 (0.06)	0.27
	0.15	0.86 (0.07)	0.85 (0.07)	0.32	0.86 (0.07)	0.83 (0.07)	0.08	0.86 (0.07)	0.84 (0.08)	0.84 (0.07)	0.28
	0.18	0.84 (0.08)	0.83 (0.08)	0.35	0.84 (0.08)	0.82 (0.08)	0.09	0.84 (0.07)	0.82 (0.09)	0.82 (0.07)	0.30
	0.20	0.83 (0.08)	0.82 (0.08)	0.37	0.83 (0.08)	0.80 (0.08)	0.09	0.83 (0.08)	0.81 (0.09)	0.80 (0.08)	0.31
	0.00	1.07 (0.05)	1.09 (0.06)	0.01[§]	1.08 (0.05)	1.11 (0.06)	0.006[§]	1.08 (0.06)	1.10 (0.06)	1.11 (0.05)	0.02
	0.03	1.09 (0.06)	1.12 (0.07)	0.01[§]	1.10 (0.06)	1.13 (0.07)	0.009[§]	1.10 (0.07)	1.13 (0.07)	1.13 (0.06)	0.03
Global efficiency (SD)	0.06	1.11 (0.07)	1.14 (0.08)	0.02[§]	1.13 (0.07)	1.16 (0.08)	0.01[§]	1.13 (0.08)	1.15 (0.08)	1.16 (0.07)	0.03
	0.09	1.14 (0.08)	1.17 (0.09)	0.03	1.15 (0.09)	1.19 (0.09)	0.01[§]	1.15 (0.09)	1.18 (0.09)	1.19 (0.08)	0.05
	0.12	1.17 (0.10)	1.20 (0.10)	0.05	1.18 (0.10)	1.23 (0.10)	0.01[§]	1.18 (0.10)	1.22 (0.11)	1.22 (0.09)	0.08
	0.15	1.20 (0.11)	1.24 (0.12)	0.06	1.22 (0.11)	1.27 (0.11)	0.01[§]	1.22 (0.11)	1.25 (0.12)	1.26 (0.10)	0.09
	0.18	1.24 (0.12)	1.28 (0.13)	0.08	1.25 (0.12)	1.31 (0.12)	0.01[§]	1.26 (0.12)	1.29 (0.14)	1.30 (0.11)	0.12
	0.20	1.27 (0.13)	1.31 (0.14)	0.09	1.28 (0.13)	1.34 (0.13)	0.01[§]	1.28 (0.13)	1.33 (0.15)	1.33 (0.12)	0.11
Global efficiency (SD)	0.00	0.96 (0.02)	0.94 (0.03)	0.01[§]	0.95 (0.03)	0.93 (0.03)	0.006[§]	0.95 (0.03)	0.94 (0.03)	0.94 (0.03)	0.02
	0.03	0.95 (0.03)	0.93 (0.03)	0.01[§]	0.94 (0.03)	0.92 (0.03)	0.009[§]	0.94 (0.03)	0.93 (0.03)	0.93 (0.03)	0.03
	0.06	0.93 (0.03)	0.92 (0.04)	0.02[§]	0.93 (0.04)	0.91 (0.04)	0.01[§]	0.93 (0.04)	0.91 (0.04)	0.91 (0.03)	0.04
	0.09	0.92 (0.04)	0.90 (0.04)	0.04	0.91 (0.04)	0.89 (0.04)	0.01[§]	0.91 (0.04)	0.90 (0.05)	0.90 (0.04)	0.06
	0.12	0.90 (0.05)	0.89 (0.05)	0.06	0.90 (0.05)	0.87 (0.05)	0.01[§]	0.90 (0.05)	0.88 (0.05)	0.88 (0.04)	0.08
	0.15	0.89 (0.05)	0.87 (0.06)	0.09	0.88 (0.05)	0.86 (0.05)	0.02[§]	0.88 (0.05)	0.86 (0.06)	0.86 (0.05)	0.10
Global efficiency (SD)	0.18	0.87 (0.06)	0.85 (0.06)	0.11	0.86 (0.06)	0.84 (0.06)	0.02[§]	0.86 (0.06)	0.84 (0.07)	0.84 (0.06)	0.14
	0.20	0.85 (0.06)	0.84 (0.07)	0.13	0.85 (0.07)	0.82 (0.06)	0.03[§]	0.85 (0.06)	0.83 (0.07)	0.83 (0.06)	0.15

Table 4 continued

Metric	Correlation threshold	Healthy controls	MS patients	p^*	CP MS patients	CI MS patients	p^*	RRMS patients	SPMS patients	BMS patients	p^*	
Local efficiency (SD)	0.00	0.97 (0.02)	0.96 (0.02)	0.12	0.96 (0.02)	0.95 (0.02)	0.05	0.96 (0.02)	0.96 (0.02)	0.96 (0.02)	0.17	
	0.03	0.96 (0.02)	0.95 (0.02)	0.16	0.96 (0.02)	0.95 (0.03)	0.06	0.96 (0.02)	0.95 (0.03)	0.95 (0.02)	0.18	
	0.06	0.95 (0.02)	0.95 (0.03)	0.20	0.95 (0.03)	0.94 (0.03)	0.07	0.95 (0.02)	0.94 (0.03)	0.94 (0.02)	0.21	
	0.09	0.95 (0.03)	0.94 (0.03)	0.23	0.94 (0.03)	0.93 (0.03)	0.07	0.94 (0.03)	0.94 (0.03)	0.94 (0.03)	0.22	
	0.12	0.94 (0.03)	0.93 (0.03)	0.25	0.94 (0.03)	0.93 (0.03)	0.06	0.94 (0.03)	0.93 (0.04)	0.93 (0.03)	0.24	
	0.15	0.93 (0.03)	0.92 (0.04)	0.28	0.93 (0.04)	0.92 (0.04)	0.07	0.93 (0.03)	0.92 (0.04)	0.92 (0.03)	0.25	
	0.18	0.92 (0.04)	0.91 (0.04)	0.28	0.92 (0.04)	0.91 (0.04)	0.07	0.92 (0.04)	0.91 (0.04)	0.91 (0.03)	0.26	
	0.20	0.91 (0.04)	0.90 (0.04)	0.29	0.91 (0.04)	0.90 (0.04)	0.07	0.91 (0.04)	0.90 (0.04)	0.90 (0.04)	0.26	
	0.00	-0.02 (0.03)	0.01 (0.04)	<0.001[§]	0.009 (0.05)	0.01 (0.04)	<0.001[§]	0.005 (0.04)	0.02 (0.04)	0.01 (0.04)	0.01 (0.04)	<0.001[§]
	0.03	-0.01 (0.03)	0.01 (0.05)	<0.001[§]	0.01 (0.05)	0.02 (0.04)	<0.001[§]	0.01 (0.05)	0.03 (0.05)	0.03 (0.05)	0.02 (0.05)	<0.001[§]
0.06	-0.01 (0.03)	0.02 (0.05)	<0.001[§]	0.02 (0.05)	0.03 (0.05)	<0.001[§]	0.02 (0.05)	0.03 (0.05)	0.03 (0.05)	0.03 (0.05)	<0.001[§]	
0.09	-0.01 (0.04)	0.03 (0.06)	<0.001[§]	0.03 (0.06)	0.04 (0.06)	<0.001[§]	0.02 (0.06)	0.04 (0.06)	0.04 (0.06)	0.03 (0.06)	<0.001[§]	
0.12	0.00 (0.04)	0.04 (0.06)	<0.001[§]	0.03 (0.06)	0.05 (0.07)	0.001[§]	0.03 (0.06)	0.05 (0.07)	0.05 (0.07)	0.05 (0.07)	0.001[§]	
0.15	0.01 (0.05)	0.05 (0.07)	0.001[§]	0.04 (0.07)	0.06 (0.07)	0.003[§]	0.04 (0.07)	0.06 (0.07)	0.06 (0.07)	0.06 (0.08)	0.004[§]	
0.18	0.02 (0.05)	0.06 (0.08)	0.004[§]	0.04 (0.07)	0.07 (0.08)	0.005[§]	0.04 (0.07)	0.07 (0.08)	0.07 (0.08)	0.07 (0.08)	0.009[§]	
0.20	0.03 (0.06)	0.06 (0.08)	0.006[§]	0.05 (0.07)	0.08 (0.08)	0.004[§]	0.05 (0.07)	0.08 (0.08)	0.08 (0.08)	0.07 (0.08)	0.01[§]	
Hierarchy (SD)	0.00	0.09 (0.06)	0.05 (0.09)	0.007	0.06 (0.11)	0.05 (0.07)	0.02	0.06 (0.09)	0.05 (0.11)	0.05 (0.08)	0.04	
	0.03	0.09 (0.06)	0.06 (0.12)	0.10	0.06 (0.10)	0.06 (0.16)	0.26	0.06 (0.09)	0.07 (0.18)	0.05 (0.08)	0.36	
	0.06	0.08 (0.06)	0.06 (0.09)	0.02	0.06 (0.10)	0.05 (0.07)	0.07	0.06 (0.09)	0.05 (0.08)	0.05 (0.08)	0.27	
	0.09	0.08 (0.07)	0.06 (0.09)	0.07	0.07 (0.09)	0.04 (0.08)	0.04	0.07 (0.09)	0.05 (0.08)	0.05 (0.09)	0.22	
	0.12	0.08 (0.08)	0.06 (0.09)	0.10	0.06 (0.09)	0.05 (0.10)	0.18	0.07 (0.10)	0.05 (0.08)	0.06 (0.09)	0.39	
	0.15	0.09 (0.07)	0.06 (0.09)	0.04	0.07 (0.10)	0.05 (0.08)	0.04	0.07 (0.10)	0.06 (0.09)	0.06 (0.09)	0.34	
	0.18	0.09 (0.09)	0.07 (0.09)	0.07	0.08 (0.09)	0.05 (0.08)	0.01	0.07 (0.09)	0.07 (0.09)	0.07 (0.08)	0.36	
	0.20	0.10 (0.09)	0.07 (0.09)	0.03	0.08 (0.09)	0.05 (0.08)	0.007	0.07 (0.09)	0.07 (0.09)	0.07 (0.10)	0.18	

CP cognitively preserved, CI cognitively impaired, RR relapsing remitting, BMS benign form of MS, SP secondary progressive

* ANOVA model adjusted for age and gender. Values are reported in bold when statistical significance is met. p values marked with [§]survived the correction for multiple comparisons, performed with the false discovery rate approach

Table 5 Brain hubs in healthy controls and patients with MS, as a whole and according to the presence/absence of cognitive impairment

Brain regions	Side	Integrated nodal parameter (X_{nod})							
		Healthy controls		All MS patients		CP MS patients		CI MS patients	
		k	B	k	B	k	B	k	B
ACC	L	–	5.98	–	–	–	5.38	–	–
	R	–	5.72	–	6.20	–	5.57	–	7.29
OFC	L	–	–	–	–	–	5.39	–	–
	R	–	5.05	–	6.32	–	5.93	–	7.03
SFG	L	–	5.09	–	–	–	–	–	–
ITG	L	22.00	5.68	–	6.36	–	5.70	–	7.52
	R	22.25	6.05	21.74	6.50	22.16	6.06	21.26	7.18
MTG	L	22.47	6.39	22.30	7.56	22.51	6.53	22.02	8.99
	R	22.30	6.03	22.07	6.85	22.28	6.05	21.81	7.85
<i>Superior TP</i>	<i>L</i>	–	–	–	6.12	–	5.77	–	6.81
MCC	L	22.18	5.47	–	6.31	–	5.82	–	6.93
	R	22.23	5.77	–	6.15	–	5.58	–	6.82
Precuneus	L	22.06	5.21	–	–	–	–	–	–
<i>Lingual gyrus</i>	<i>L</i>	–	–	–	–	–	–	–	6.70
Putamen	L	–	5.11	–	–	–	–	–	–
	R	–	–	–	–	–	–	–	7.49
<i>Pallidus</i>	<i>R</i>	–	–	–	6.15	–	5.98	–	–
<i>Caudate</i>	<i>L</i>	–	–	–	–	–	6.05	–	–
Thalamus	L	–	5.06	–	–	–	5.75	–	–
	R	–	–	–	6.19	–	6.26	–	–
Cerebellum (crus I)	L	22.60	6.07	21.93	6.46	22.16	5.57	21.58	7.61
	R	22.81	6.84	22.02	6.96	22.31	6.19	21.56	7.65
Cerebellum (crus II)	L	–	5.97	–	6.23	–	5.55	–	7.46
	R	–	5.45	–	–	–	–	–	–
<i>Cerebellum (lobule IV–V)</i>	<i>L</i>	–	–	–	6.01	–	–	–	6.82
<i>Cerebellum (lobule VIII)</i>	<i>R</i>	–	–	–	–	–	5.46	–	–

Hub regions identified in all groups are reported in normal text, hub regions identified in controls only are highlighted in bold; hub regions identified in patients only are reported in italics

k nodal degree, B betweenness centrality, L left, R right, CP cognitively preserved, CI cognitively impaired, ACC anterior cingulate cortex, ITG inferior temporal gyrus, MCC middle cingulate cortex, MTG middle temporal gyrus, OFC orbitofrontal cortex, TP temporal pole, PHG parahippocampal gyrus, SFG superior frontal gyrus

addition, RRMS patients had a hub distribution similar to that of HCs, apart from the loss of hubs in the left basal ganglia. BMS patients had an increased number of hubs in the bilateral cerebellum and right lingual gyrus, as well as a loss of the hub in the left ACC. SPMS patients showed a reduced number of cortical hubs, especially in the left hemisphere, which were shifted to posterior brain regions.

Compared to HCs, RRMS patients experienced a significantly lower nodal degree of the bilateral caudate nucleus ($q \leq 0.001$). A trend towards a lower nodal degree of the left caudate was also detected when comparing SPMS vs RRMS ($q = 0.004$) or BMS ($q = 0.03$) patients, and BMS vs RRMS patients ($q = 0.04$).

Network analysis and structural damage

In patients, global and regional network properties were not correlated with T2 lesion volume and normalized brain volume.

Discussion

Cortico-cortical and cortico-subcortical disconnections secondary to the involvement of white matter tracts have been consistently demonstrated by structural MRI studies of patients with MS. This architectural disruption is clinically relevant, since it was found to contribute to cognitive impairment in these patients (Dineen et al. 2009; Mesaros et al. 2012). We hypothesized that a disconnection between functionally relevant brain areas might also contribute to explain cognitive deficits of MS patients, and better characterize disease heterogeneity, in term of clinical phenotypes. To prove our hypothesis, we used a graph theoretical analysis of RS fMRI to assess global and regional topological brain functional organization in a large cohort of MS patients. The main advantage of RS fMRI analysis is that this task-free approach allows inferences related to differences between healthy and diseased subjects, which are not influenced by task performance, thus permitting the

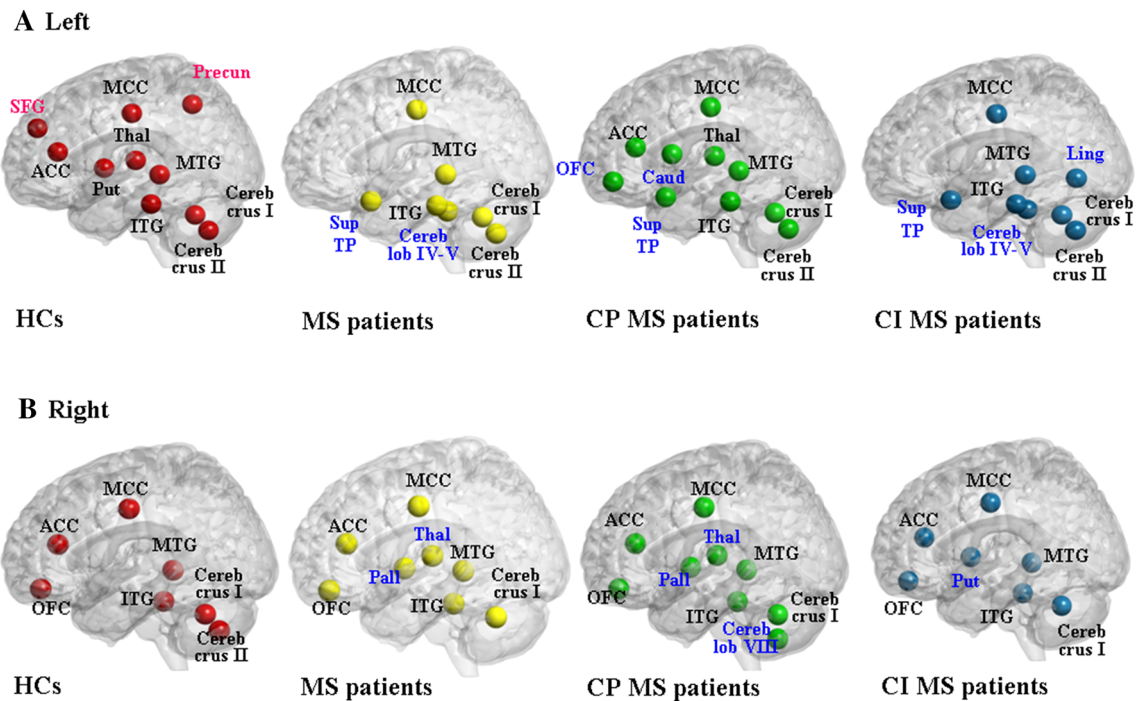


Fig. 2 Brain hubs (**a** left hemisphere, **b** right hemisphere) of the functional networks of healthy controls (HCs) and patients with MS as a whole and according to the presence/absence of cognitive impairment. Hubs were identified as brain regions having either integrated nodal degree or betweenness centrality one standard deviation greater than the network average. Hubs present in HC only are reported in *red*, hubs present in MS patients only are reported in

blue, and hubs present in all groups are reported in *black*. *CP* cognitively preserved, *CI* cognitively impaired, *ACC* anterior cingulate cortex, *Caud* caudate nucleus, *Cereb* cerebellum, *ITG* inferior temporal gyrus, *Ling* lingual gyrus, *MCC* middle cingulate cortex, *MTG* middle temporal gyrus, *OFC* orbitofrontal cortex, *Pall* pallidus, *Precun* precuneus, *Put* putamen, *SFG* superior frontal gyrus, *Sup TP* superior temporal pole, *Thal* thalamus

assessment of patients with severe clinical disability and/or cognitive deficits (Rocca et al. 2010c).

Despite maintaining small-world attributes in MS patients, a disruption of global functional organization was detected, as shown by the reduction of mean network degree, global efficiency and hierarchy, and the increase of path length and assortativity. These abnormalities of global network properties allowed us to distinguish CI MS patients from HCs and CP patients, but not the main MS clinical phenotypes. Small-world networks combine high levels of local clustering among nodes and short paths that globally link all the nodes of the network (Bullmore and Sporns 2009). The simplest global network property is the mean network degree, which is a measure of density or the total “wiring cost” of the network. Its reduction in MS patients suggests that their functional brain networks have more nodes with a few connections (low degree) and fewer nodes with many connections (high degree) compared to those of controls (Rubinov and Sporns 2010). To note, network clustering coefficient, which is a measure of functional segregation (i.e., the ability of specialized processes to occur within highly interconnected groups of brain regions), was not affected in MS patients.

Conversely, the characteristic path length and global efficiency, which are measures of functional integration (i.e., ability to rapidly combine specialized information from distributed brain regions) (Rubinov and Sporns 2010), were altered. Therefore, our results suggest a preservation of the efficiency of local information transfer and processing and an impairment of global integration, likely to reflect a reduced competence in information exchange between distant brain areas. This is also supported by the higher assortativity and lower hierarchy we found in patients’ networks. In assortative networks, nodes with many connections tend to be connected to other nodes with many connections, and nodes with low connections are linked to other low connection nodes (Newman 2002). Hierarchy is the tendency of hubs to connect to nodes that are not otherwise connected to each other (Bassett et al. 2008). Therefore, increased assortativity and reduced hierarchy indicate an impaired wiring efficiency at a system level. Conceivably, this is likely to contribute to explain cognitive impairment in MS patients (since cognition depends on coordinated interactions among many brain regions). Abnormalities of these two metrics also point to a tendency to form subnetworks of highly

Table 6 Results of the comparison of nodal degree between healthy controls and patients with MS, as a whole and according to the presence/absence of cognitive impairment

Brain regions	Side	Integrated nodal parameter (X_{nod}) for degree		q values*
		Healthy controls	All MS patients	
Caudate nucleus	R	13.70	5.75	1.7×10^{-10}
Caudate nucleus	L	17.50	11.40	6.9×10^{-8}
Cerebellum (crus I)	R	22.81	22.02	0.001
		Healthy controls	CP MS patients	
Caudate nucleus	R	13.70	5.96	2×10^{-9}
Caudate nucleus	L	17.50	12.03	2×10^{-6}
		Healthy controls	CI MS patients	
Caudate nucleus	R	13.70	5.58	4×10^{-10}
Caudate nucleus	L	17.50	10.25	2×10^{-9}
Cerebellum (crus I)	R	22.81	21.56	2×10^{-4}
Anterior cingulate cortex	L	21.72	19.64	3×10^{-4}
Thalamus	L	19.90	17.09	0.001
Cerebellum (lobule VIII)	R	21.75	19.78	0.001
Superior frontal gyrus	L	21.55	19.53	0.001
Precuneus	L	22.06	20.66	0.001
Heschl's gyrus	L	20.08	16.99	0.001

The nodal parameter for degree (X_{nod}) is obtained by integrating all degree values over the range of considered correlation thresholds ($0 \leq \tau \leq 0.20$). Correction for multiple comparisons was performed by controlling for the positive false discovery rate (pFDR). Brain regions were ranked according to their importance in explaining group differences by means of their q value (i.e., the pFDR analogue of the p value)

* Statistical analysis: q value, controlling for positive false discovery rate (pFDR)

connected core regions (Bassett et al. 2008; Newman 2002), which might be protected from being injured due to redundant connections (Newman 2002).

Abnormalities of network properties similar to those we have found in MS patients have been described in patients with schizophrenia and have contributed to support the hypothesis of schizophrenia as a disconnection syndrome (Bassett et al. 2008). Conversely, the only study that has assessed, so far, a few of these network metrics in a small group of MS patients (Schoonheim et al. 2011) found no abnormalities of clustering coefficient and a reduced path length in male patients only. Differences in number of subjects enrolled (only 15 subjects in Schoonheim et al. 2011), and analysis methods (Pearson's

correlation vs synchronization likelihood; computation of network average degree vs use of correlation threshold) are likely to account for differences between ours and previous results.

The analysis of network organization at a regional level allowed us to identify the nodes with a different role in MS patients vs HC, not only in term of a qualitative difference in hub distribution, but also of a reduced functional connectivity of strategic brain regions. Independent of cognitive status and disease phenotype, the hallmarks of hubs distribution in MS patients were: (1) a loss of hubs in the SFG, precuneus and ACC in the left hemisphere; (2) a different lateralization of basal ganglia hubs; and (3) a formation of hubs, which were not seen in HCs, in the left temporal pole and cerebellar lobule IV–V. A decreased nodal degree was found in the bilateral caudate nucleus and right cerebellum.

The precuneus, SFG and ACC are part of the default mode network (DMN). Disruption of DMN functional connectivity has been associated with cognitive deficits in elderly individuals (Damoiseaux et al. 2008) and MS patients (Rocca et al. 2010c). The precuneus and the surrounding posterior cingulate cortex are among the brain regions with the highest metabolic rates at rest (Cavanna and Trimble 2006), and have been shown to compose the structural core of the human brain (Hagmann et al. 2008). This functional/anatomical correspondence has led to the hypothesis that core regions of the parietal lobe may be the basis for shaping large-scale brain dynamics (Hagmann et al. 2008). Anatomically, the principal extraparietal cortico-cortical connections of the precuneus are with regions of the frontal (prefrontal cortex and ACC) and temporal (associative cortex in the superior temporal sulcus) lobes, and its subcortical connections are with the thalamus, caudate nucleus and putamen (Cavanna and Trimble 2006). Through connections with the pons, the precuneus can also gain access to multiple cerebellar circuits. Hence, our findings suggest a disruption of functional interactions of cortical and subcortical structures of this network, which is thought to be involved in elaborating integrated and associative information.

Such an impairment of regional network properties was found to contribute to cognitive impairment and phenotypic variability of MS patients. Hub distribution was relatively intact in CP patients, who also were found to harbour additional hubs in the cerebellum, orbitofrontal cortex and caudate nucleus. Conversely, CI patients did not have hubs in the thalamus and left frontal lobes. The lack of frontal lobe hubs in CI MS patients agrees with the results of several previous active fMRI studies, which have consistently demonstrated an increased recruitment of regions located in the frontal lobes. These studies also suggested that an increased functional connectivity

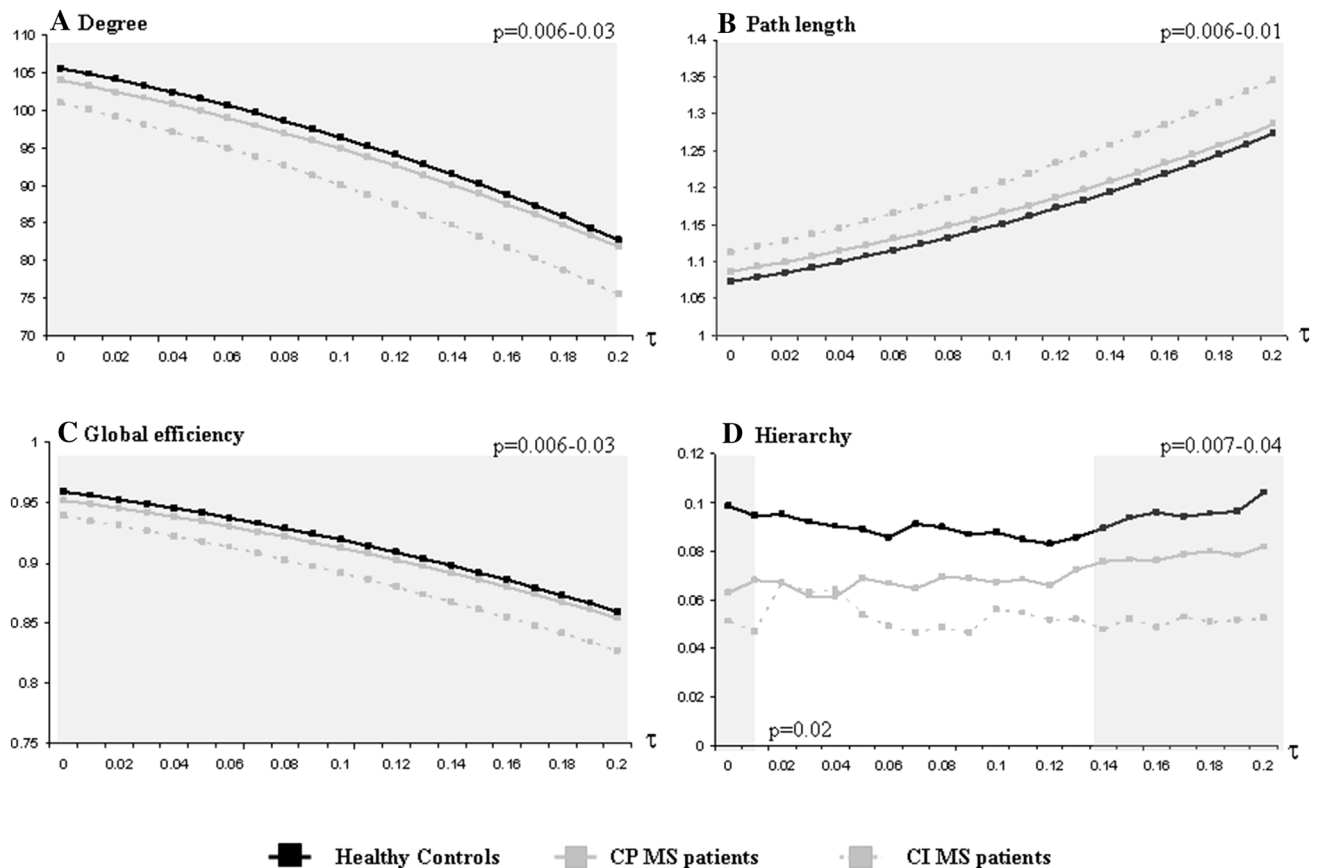


Fig. 3 Plots of the global network properties significantly different between healthy controls (black line), cognitively preserved (CP) patients with MS (continuous grey line) and cognitively impaired (CI) MS patients (dashed grey lines) over the selected range of correlation

thresholds τ : **a** mean network degree; **b** characteristic path length; **c** global efficiency; and **d** hierarchy. Shade areas indicate the range of thresholds where between-group differences were statistically significant

between frontal regions may represent a compensatory mechanism contributing to a preserved cognitive performance (Bonnet et al. 2010; Rocca et al. 2010b; Staffen et al. 2002). Thalamic involvement has been associated with many clinical manifestations of MS, including fatigue, and cognitive and motor deficits (Minagar et al. 2013). However, while several studies have investigated the contribution of thalamic structural damage to MS clinical manifestations (Minagar et al. 2013), this is one of the first studies showing that functional loss of the thalamic connector is associated with MS cognitive impairment. In addition, it suggests that the redistribution of functional hubs can be functionally ineffective or associated with more severe clinical manifestations (probably reflecting a maladaptive mechanism). This is the case, for instance, for the hubs located in the cerebellum and lingual gyrus in CI patients. An impaired functional connectivity between the cerebellum and the frontal lobes has been shown to contribute to failure of cognitive compensation in MS patients (Bonnet et al. 2010); on the contrary, an increased recruitment of

posterior brain regions and the cerebellum has been detected in CI patients with primary progressive MS (Rocca et al. 2010b).

While the analysis of global network properties was not informative to explain clinical phenotypic variability, abnormalities of hub distribution contributed to better characterize the main MS clinical phenotypes. Indeed, this analysis revealed that RRMS patients retained the majority of hubs, while SPMS experienced the formation of several additional hubs in the posterior regions of the brain and cerebellum, and a hub loss in the left frontal lobe and along the cingulum. This suggests that loss of “critical” hubs and functional incompetence of alternative hubs may contribute to a progressive disease course. Finally, patients with BMS had a pattern of hub distribution somewhat between those of RRMS and SPMS patients, with a preservation of the hub in the left middle cingulum, and several additional hubs in the cerebellum, bilaterally. The capability to maintain over time the functional integrity and specialization of specific brain regions might be among the factors responsible for the

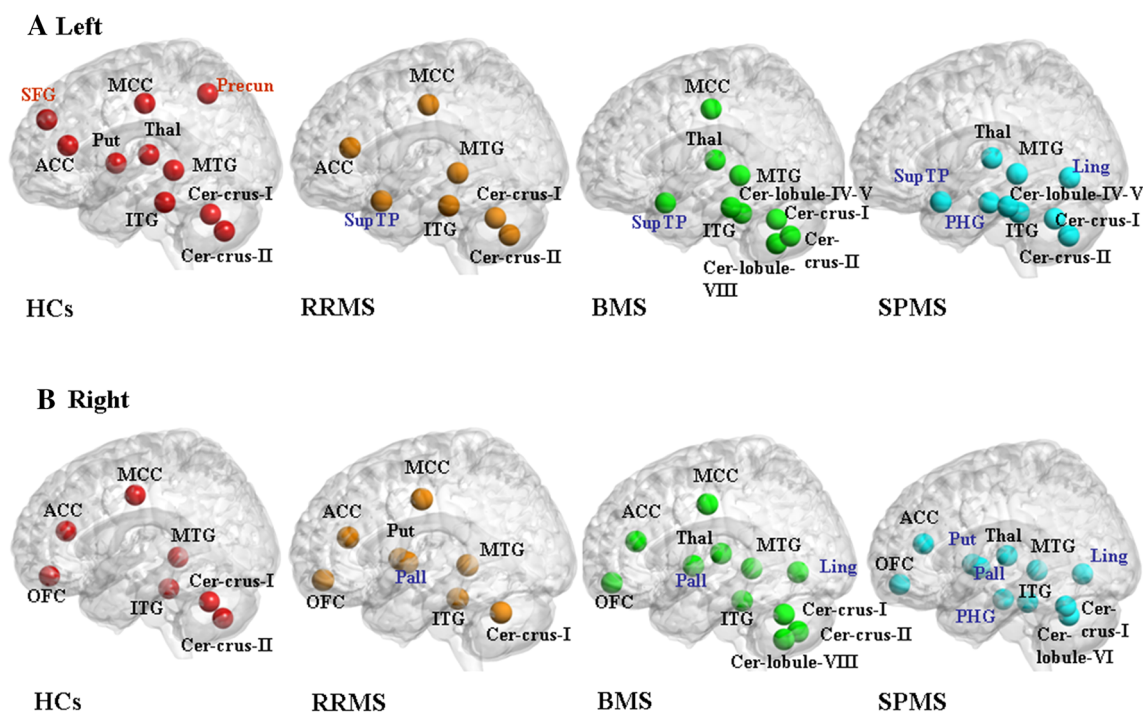


Fig. 4 Brain hubs (**a** left hemisphere, **b** right hemisphere) of the functional networks of healthy controls (HCs) and patients with different MS clinical phenotypes. Hubs were identified as brain regions having either integrated nodal degree or betweenness centrality one standard deviation greater than the network average. Hubs present in HC only are reported in *red*, hubs present in MS patients only are reported in *blue*, and hubs present in all groups are

reported in *black*. RRMS relapsing remitting MS, BMS benign MS, SPMS secondary progressive MS, ACC anterior cingulate cortex, *Caud* caudate nucleus, *Cer* cerebellum, *ITG* inferior temporal gyrus, *Ling* lingual gyrus, *MCC* middle cingulate cortex, *MTG* middle temporal gyrus, *OFC* orbitofrontal cortex, *Pall* pallidus, *PHG* parahippocampal gyrus, *Precun* precuneus, *Put* putamen, *SFG* superior frontal gyrus, *Sup TP* superior temporal pole, *Thal* thalamus

favourable clinical course of BMS, and agrees with the results of previous active motor and cognitive fMRI studies (Rocca et al. 2009, 2010a, 2012). Notably, regional modifications of network organization correlated to phenotypic variability had only a partial overlap with those associated with cognitive impairment, indicating the importance of functional abnormalities at a regional level in explaining the various clinical manifestations of MS.

This study is not without limitations. First, the cross-sectional design did not allow us to assess the temporal dynamics of the detected functional abnormalities and how they might eventually impact the development of cognitive deficits or the evolution to a different disease clinical phenotype. Second, cognitive impairment was defined based on the performance at PASAT and not on a comprehensive neuropsychological evaluation. Nevertheless, PASAT has been shown to be sensitive to abnormalities of working memory and information processing speed which are among the most frequently affected cognitive domains in MS. Third, the topological organization of brain networks has been shown to be affected by

the parcellation strategies applied (de Reus and van den Heuvel 2013), the measure used to assess functional coupling between RS fMRI time series (Zalesky et al. 2012), and the metric used to assess node centrality (Zuo et al. 2012). As a consequence, we cannot exclude that the use of another atlas, a different parcellation method, another coupling metric (e.g., partial correlation (Salvador et al. 2005), synchronization likelihood (Schoonheim et al. 2011) or wavelet analysis (Bassett et al. 2008)), or another centrality measure (e.g., eigenvector centrality) (Lohmann et al. 2010) would have resulted in different characterization of network properties. Fourth, to investigate the influence of structural disease-related damage on functional network parameters we used only T2 lesion volumes and brain atrophy. Future studies using advanced structural MRI techniques, such as diffusion tensor or magnetization transfer MRI, might be more helpful to investigate associations between microstructural damage and functional network abnormalities and their interplay in the different stages of the disease. Even if it is a challenging task, due to the presence of systems interconnected by polysynaptic circuitry, further graph

Table 7 Brain hubs in healthy controls and patients with MS and different phenotypes

Brain regions	Side	Integrated nodal parameter (X_{nod})							
		Healthy controls		RRMS patients		BMS patients		SPMS patients	
		<i>k</i>	<i>B</i>	<i>k</i>	<i>B</i>	<i>k</i>	<i>B</i>	<i>k</i>	<i>B</i>
ACC	L	–	5.98	–	5.52	–	–	–	–
	R	–	5.72	–	5.69	–	6.75	–	6.66
OFC	R	–	5.05	–	5.83	–	7.06	–	6.65
SFG	L	–	5.09	–	–	–	–	–	–
ITG	L	22.00	5.68	–	6.10	–	6.57	–	6.64
	R	22.25	6.05	22.05	6.10	21.56	7.04	21.39	6.80
MTG	L	22.47	6.39	22.52	6.76	22.09	8.40	22.08	8.31
	R	22.30	6.03	22.33	6.36	21.74	7.15	21.87	7.41
<i>Superior TP</i>	<i>L</i>	–	–	–	5.53	–	7.42	–	6.27
MCC	L	22.18	5.47	–	6.04	–	7.21	–	–
	R	22.23	5.77	–	5.92	–	6.84	–	–
Precuneus	L	22.06	5.21	–	–	–	–	–	–
<i>Lingual gyrus</i>	<i>L</i>	–	–	–	–	–	–	–	6.79
	<i>R</i>	–	–	–	–	–	6.50	–	6.64
<i>PHG</i>	<i>L</i>	–	–	–	–	–	–	–	6.25
	<i>R</i>	–	–	–	–	–	–	–	6.42
Putamen	L	–	5.11	–	–	–	–	–	–
	R	–	–	–	5.69	–	–	–	6.32
<i>Pallidus</i>	<i>R</i>	–	–	–	5.74	–	6.59	–	6.52
<i>Caudate</i>	<i>L</i>	–	–	–	–	–	6.73	–	–
Thalamus	L	–	5.06	–	–	–	7.19	–	6.76
	R	–	–	–	–	–	7.29	–	6.76
Cerebellum (crus I)	L	22.60	6.07	22.08	5.52	21.68	7.01	21.85	7.59
	R	22.81	6.84	22.32	6.45	21.83	7.87	21.67	7.21
Cerebellum (crus II)	L	–	5.97	–	5.84	–	7.29	–	6.24
	R	–	5.45	–	–	–	6.46	–	–
<i>Cerebellum (lobule VI)</i>	<i>R</i>	–	–	–	–	–	–	–	6.32
<i>Cerebellum (lobule IV–V)</i>	<i>L</i>	–	–	–	–	–	6.70	–	6.74
<i>Cerebellum (lobule VIII)</i>	<i>L</i>	–	–	–	–	–	6.62	–	–
	<i>R</i>	–	–	–	–	–	6.68	–	–

Hub regions identified in controls only are highlighted in bold; hub regions identified in patients only are reported in italics

k degree, *B* betweenness centrality, *L* left, *R* right, *RRMS* relapsing remitting MS, *BMS* benign MS, *SPMS* secondary progressive MS, *ACC* anterior cingulate cortex, *ITG* inferior temporal gyrus, *MCC* middle cingulate cortex, *MTG* middle temporal gyrus, *OFC* orbitofrontal cortex, *TP* temporal pole, *PHG* parahippocampal gyrus, *SFG* superior frontal gyrus

analysis studies are warranted to determine the relationship between structural and functional connectivity abnormalities in these patients.

Acknowledgments We wish to thank Dr. Sara Sala for her help in conducting the statistical analysis. This work has been partially supported by a grant from Fondazione Italiana Sclerosi Multipla (FISM/2011/R/19) and by a grant from Italian Ministry of Health (GR-2009-1529671).

Conflict of interest The authors declare that they have no conflict of interest.

References

- Amato MP, Portaccio E, Goretti B, Zipoli V, Ricchiuti L, De Caro MF, Patti F, Vecchio R, Sorbi S, Trojano M (2006) The Rao's brief repeatable battery and stroop test: normative values with age, education and gender corrections in an Italian population. *Mult Scler* 12:787–793
- Ashburner J, Friston KJ (1999) Nonlinear spatial normalization using basis functions. *Hum Brain Mapp* 7:254–266
- Bassett DS, Bullmore E, Verchinski BA, Mattay VS, Weinberger DR, Meyer-Lindenberg A (2008) Hierarchical organization of human cortical networks in health and schizophrenia. *J Neurosci* 28:9239–9248
- Benjamini Y, Hochberg Y (1995) Controlling the false discovery rate: a practical and powerful approach to multiple testing. *J R Stat Soc Ser B* 57:289–300
- Bonnet MC, Allard M, Dilharreguy B, Deloire M, Petry KG, Brochet B (2010) Cognitive compensation failure in multiple sclerosis. *Neurology* 75:1241–1248
- Bullmore E, Sporns O (2009) Complex brain networks: graph theoretical analysis of structural and functional systems. *Nat Rev Neurosci* 10:186–198
- Cavanna AE, Trimble MR (2006) The precuneus: a review of its functional anatomy and behavioural correlates. *Brain* 129:564–583

- Damoiseaux JS, Beckmann CF, Arigita EJ, Barkhof F, Scheltens P, Stam CJ, Smith SM, Rombouts SA (2008) Reduced resting-state brain activity in the “default network” in normal aging. *Cereb Cortex* 18:1856–1864
- de Haan W, Pijnenburg YA, Strijers RL, van der Made Y, van der Flier WM, Scheltens P, Stam CJ (2009) Functional neural network analysis in frontotemporal dementia and Alzheimer’s disease using EEG and graph theory. *BMC Neurosci* 10:101
- de Reus MA, van den Heuvel MP (2013) The parcellation-based connectome: limitations and extensions. *Neuroimage* 80:397–404
- Diedrichsen J, Verstynen T, Schlerf J, Wiestler T (2010) Advances in functional imaging of the human cerebellum. *Curr Opin Neurol* 23:382–387
- Dineen RA, Vilisaar J, Hlinka J, Bradshaw CM, Morgan PS, Constantinescu CS, Auer DP (2009) Disconnection as a mechanism for cognitive dysfunction in multiple sclerosis. *Brain* 132:239–249
- Filippi M, van den Heuvel MP, Fornito A, He Y, Hulshoff Pol HE, Agosta F, Comi G, Rocca MA (2013) Assessment of system dysfunction in the brain through MRI-based connectomics. *Lancet Neurol* 12:1189–1199
- Fischer JS, Rudick RA, Cutter GR, Reingold SC (1999) The multiple sclerosis functional composite measure (MSFC): an integrated approach to MS clinical outcome assessment. National MS society clinical outcomes assessment task force. *Mult Scler* 5:244–250
- Hagmann P, Cammoun L, Gigandet X, Meuli R, Honey CJ, Wedeen VJ, Sporns O (2008) Mapping the structural core of human cerebral cortex. *PLoS Biol* 6:e159
- Hawkins SA, McDonnell GV (1999) Benign multiple sclerosis? Clinical course, long term follow up, and assessment of prognostic factors. *J Neurol Neurosurg Psychiatry* 67:148–152
- He Y, Chen Z, Evans A (2008) Structural insights into aberrant topological patterns of large-scale cortical networks in Alzheimer’s disease. *J Neurosci* 28:4756–4766
- He Y, Dagher A, Chen Z, Charil A, Zijdenbos A, Worsley K, Evans A (2009) Impaired small-world efficiency in structural cortical networks in multiple sclerosis associated with white matter lesion load. *Brain* 132:3366–3379
- Humphries MD, Gurney K, Prescott TJ (2006) The brainstem reticular formation is a small-world, not scale-free, network. *Proc Biol Sci* 273:503–511
- Latora V, Marchiori M (2001) Efficient behavior of small-world networks. *Phys Rev Lett* 87:198701
- Li Y, Jewells V, Kim M, Chen Y, Moon A, Armao D, Troiani L, Markovic-Plese S, Lin W, Shen D (2013) Diffusion tensor imaging based network analysis detects alterations of neuroconnectivity in patients with clinically early relapsing-remitting multiple sclerosis. *Hum Brain Mapp* 34:3376–3391
- Lohmann G, Margulies DS, Horstmann A, Pleger B, Lepsien J, Goldhahn D, Schloegl H, Stumvoll M, Villringer A, Turner R (2010) Eigenvector centrality mapping for analyzing connectivity patterns in fMRI data of the human brain. *PLoS ONE* 5:e10232
- Lublin FD, Reingold SC (1996) Defining the clinical course of multiple sclerosis: results of an international survey. National multiple sclerosis society (USA) advisory committee on clinical trials of new agents in multiple sclerosis. *Neurology* 46:907–911
- Lund TE, Norgaard MD, Rostrup E, Rowe JB, Paulson OB (2005) Motion or activity: their role in intra- and inter-subject variation in fMRI. *Neuroimage* 26:960–964
- Maslov S, Sneppen K (2002) Specificity and stability in topology of protein networks. *Science* 296:910–913
- Mesaros S, Rocca MA, Kacar K, Kostic J, Copetti M, Stosic-Opincal T, Preziosa P, Sala S, Riccitelli G, Horsfield MA, Drulovic J, Comi G, Filippi M (2012) Diffusion tensor MRI tractography and cognitive impairment in multiple sclerosis. *Neurology* 78:969–975
- Meunier D, Achard S, Morcom A, Bullmore E (2009) Age-related changes in modular organization of human brain functional networks. *Neuroimage* 44:715–723
- Minagar A, Barnett MH, Benedict RH, Pelletier D, Pirko I, Sahraian MA, Frohman E, Zivadinov R (2013) The thalamus and multiple sclerosis: modern views on pathologic, imaging, and clinical aspects. *Neurology* 80:210–219
- Newman ME (2002) Assortative mixing in networks. *Phys Rev Lett* 89:208701
- Polman CH, Reingold SC, Banwell B, Clanet M, Cohen JA, Filippi M, Fujihara K, Havrdova E, Hutchinson M, Kappos L, Lublin FD, Montalban X, O’Connor P, Sandberg-Wollheim M, Thompson AJ, Waubant E, Weinschenker B, Wolinsky JS (2011) Diagnostic criteria for multiple sclerosis: 2010 revisions to the McDonald criteria. *Ann Neurol* 69:292–302
- Ravasz E, Barabasi AL (2003) Hierarchical organization in complex networks. *Phys Rev E: Stat Nonlin Soft Matter Phys* 67:026112
- Rocca MA, Valsasina P, Ceccarelli A, Absinta M, Ghezzi A, Riccitelli G, Pagani E, Falini A, Comi G, Scotti G, Filippi M (2009) Structural and functional MRI correlates of Stroop control in benign MS. *Hum Brain Mapp* 30:276–290
- Rocca MA, Ceccarelli A, Rodegher M, Misci P, Riccitelli G, Falini A, Comi G, Filippi M (2010a) Preserved brain adaptive properties in patients with benign multiple sclerosis. *Neurology* 74:142–149
- Rocca MA, Riccitelli G, Rodegher M, Ceccarelli A, Falini A, Falautano M, Meani A, Comi G, Filippi M (2010b) Functional MR imaging correlates of neuropsychological impairment in primary-progressive multiple sclerosis. *AJNR Am J Neuroradiol* 31:1240–1246
- Rocca MA, Valsasina P, Absinta M, Riccitelli G, Rodegher ME, Misci P, Rossi P, Falini A, Comi G, Filippi M (2010c) Default-mode network dysfunction and cognitive impairment in progressive MS. *Neurology* 74:1252–1259
- Rocca MA, Bonnet MC, Meani A, Valsasina P, Colombo B, Comi G, Filippi M (2012) Differential cerebellar functional interactions during an interference task across multiple sclerosis phenotypes. *Radiology* 265:864–873
- Rubinov M, Sporns O (2010) Complex network measures of brain connectivity: uses and interpretations. *Neuroimage* 52:1059–1069
- Sala S, Quatto P, Valsasina P, Agosta F, Filippi M (2014) pFDR and pFNR estimation for brain networks construction. *Stat Med* 33:158–169
- Salvador R, Suckling J, Coleman MR, Pickard JD, Menon D, Bullmore E (2005) Neurophysiological architecture of functional magnetic resonance images of human brain. *Cereb Cortex* 15:1332–1342
- Sanz-Arigita EJ, Schoonheim MM, Damoiseaux JS, Rombouts SA, Maris E, Barkhof F, Scheltens P, Stam CJ (2010) Loss of ‘small-world’ networks in Alzheimer’s disease: graph analysis of FMRI resting-state functional connectivity. *PLoS ONE* 5:e13788
- Schoonheim MM, Hulst HE, Landi D, Ciccarelli O, Roosendaal SD, Sanz-Arigita EJ, Vrenken H, Polman CH, Stam CJ, Barkhof F, Geurts JJ (2011) Gender-related differences in functional connectivity in multiple sclerosis. *Mult Scler* 18:164–173
- Shu N, Liu Y, Li K, Duan Y, Wang J, Yu C, Dong H, Ye J, He Y (2011) Diffusion tensor tractography reveals disrupted topological efficiency in white matter structural networks in multiple sclerosis. *Cereb Cortex* 21:2565–2577
- Smith SM (2002) Fast robust automated brain extraction. *Hum Brain Mapp* 17:143–155
- Staffen W, Mair A, Zauner H, Unterrainer J, Niederhofer H, Kutzelnigg A, Ritter S, Golaszewski S, Iglseder B, Ladurner G

- (2002) Cognitive function and fMRI in patients with multiple sclerosis: evidence for compensatory cortical activation during an attention task. *Brain* 125:1275–1282
- Storey JD (2003) The positive false discovery rate: a Bayesian interpretation and the q-value. *Ann Stat* 31:2013–2035
- Tian L, Wang J, Yan C, He Y (2011) Hemisphere- and gender-related differences in small-world brain networks: a resting-state functional MRI study. *Neuroimage* 54:191–202
- Tzourio-Mazoyer N, Landeau B, Papathanassiou D, Crivello F, Etard O, Delcroix N, Mazoyer B, Joliot M (2002) Automated anatomical labeling of activations in SPM using a macroscopic anatomical parcellation of the MNI MRI single-subject brain. *Neuroimage* 15:273–289
- van den Heuvel MP, Stam CJ, Kahn RS, Hulshoff Pol HE (2009) Efficiency of functional brain networks and intellectual performance. *J Neurosci* 29:7619–7624
- van Wijk BC, Stam CJ, Daffertshofer A (2010) Comparing brain networks of different size and connectivity density using graph theory. *PLoS ONE* 5:e13701
- Watts DJ, Strogatz SH (1998) Collective dynamics of ‘small-world’ networks. *Nature* 393:440–442
- Yao Z, Zhang Y, Lin L, Zhou Y, Xu C, Jiang T (2010) Abnormal cortical networks in mild cognitive impairment and Alzheimer’s disease. *PLoS Comput Biol* 6:e1001006
- Zalesky A, Fornito A, Bullmore E (2012) On the use of correlation as a measure of network connectivity. *Neuroimage* 60:2096–2106
- Zuo XN, Ehmke R, Mennes M, Imperati D, Castellanos FX, Sporns O, Milham MP (2012) Network centrality in the human functional connectome. *Cereb Cortex* 22:1862–1875